Article:
Roy, Soumya S. orcid.org/0000-0002-9193-9712, Stevanato, Gabriele, Rayner, Peter J. orcid.org/0000-0002-6577-4117 et al. (1 more author) (2017) Direct enhancement of nitrogen-15 targets at high-field by fast ADAPT-SABRE. Journal of Magnetic Resonance. YJMRE6177. pp. 55-60. ISSN 1090-7807

https://doi.org/10.1016/j.jmr.2017.10.006

Elsevier Editorial System(tm) for Journal of Magnetic Resonance

Manuscript Draft

Manuscript Number: JMR-17-254R1

Title: Direct Enhancement of Nitrogen-15 Targets at High-field by Fast ADAPT-SABRE

Article Type: Communication

Keywords: Hyperpolarization; PHIP; SABRE; ADAPT.

Corresponding Author: Professor Simon B. Duckett, BSc, PhD

Corresponding Author's Institution: Univeristy of York

First Author: Soumya Singha Roy, Ph.D.

Order of Authors: Soumya Singha Roy, Ph.D.; Gabriele Stevanato, Ph.D.; Peter J Rayner, Ph.D.; Simon B Duckett, Ph.D.

Abstract: Signal Amplification by Reversible Exchange (SABRE) is an attractive nuclear spin hyperpolarization technique capable of huge sensitivity enhancement in nuclear magnetic resonance (NMR) detection. The resonance condition of SABRE hyperpolarization depends on coherent spin mixing, which can be achieved naturally at a low magnetic field. The optimum transfer field to spin-1/2 heteronuclei is technically demanding, as it requires field strengths weaker than the earth's magnetic field for efficient spin mixing. In this paper, we illustrate an approach to achieve strong 15N SABRE hyperpolarization at high magnetic field by a radio frequency (RF) driven coherent transfer mechanism based on alternate pulsing and delay to achieve polarization transfer. The presented scheme is found to be highly robust and much faster than existing related methods, producing ~ 3 orders of 15N signal enhancement within 2 seconds of RF pulsing.

Cover Letter

THE UNIVERSITY of York

CENTRE FOR HYPERPOLARISATION IN MAGNETIC RESONANCE
Department of chemistry
York Science Park
Heslington, York, YO10 5NY, UK
Telephone: +44(0)1904 328886
www.york.ac.uk/chemistry
www.york.ac.uk/chym/

Director:
Professor Simon B. Duckett
E-mail: simon.duckett@york.ac.uk

Prof. Lucio Frydman
Editor, Journal of Magnetic Resonance

11-10-2017

Dear Lucio

Please find attached a revised manuscript entitled “Direct Enhancement of Nitrogen-15 Targets at High-field by Fast ADAPT-SABRE”, by S. S. Roy, G. Stevanato, and S. B. Duckett.

We thank you for your attention and hope that publication in the Journal of Magnetic Resonance is now possible.

Sincerely,
Simon B. Duckett

*Graphical Abstract (for review)

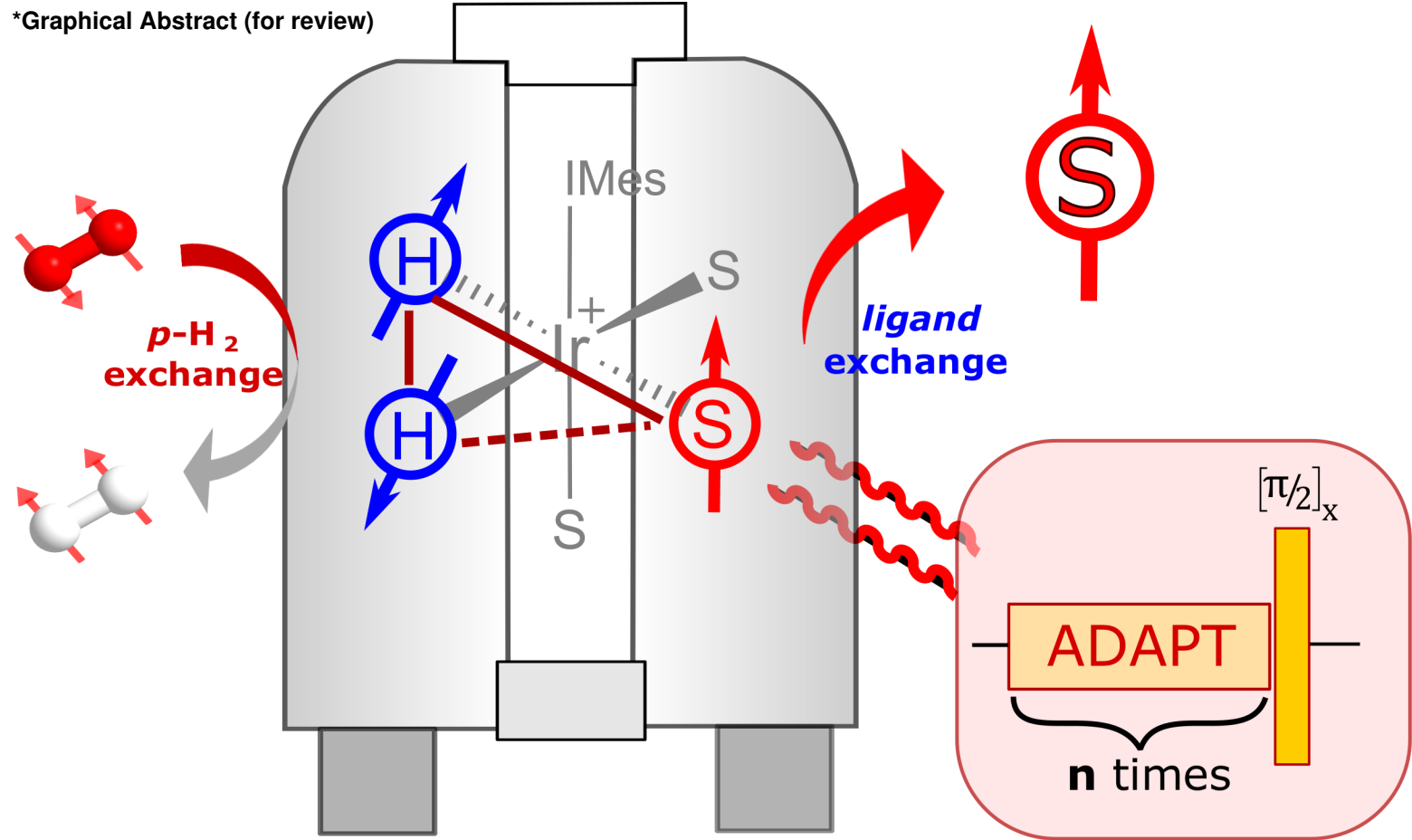

***Highlights (for review)**

Highlights

- SABRE hyperpolarization is achieved at high field by the ADAPT pulse sequence.
- A theoretical description of ADAPT-SABRE is linked to related methods for comparison.
- ADAPT-SABRE is found to achieve faster magnetization transfer than several analogous approaches.
- An optimized pulse sequence delivers nearly 3 orders of signal enhancement in 1.6 s for a 15N target.

*Response to Reviews

JMR-17-254

Reviewer #1:

[1] In section 2.1 the very first equation presenting the H_J Hamiltonian should have a number (consequently, equation numbering should be changed as well).

Equation numberings are now corrected.

[2] When writing about "optimized parameters for ADAPT" (e.g., 2nd paragraph on p. 5) please explain how exactly the optimization was done. This is necessary because (i) the choice of alpha=30^\circ is not explained (why is it 30 but not some other angle?) and (ii) the choice of \Delta and m is not unique (as written in Section 2.2).

(i) The choice of alpha = 30^\circ was based on a series of measurements and this led to an optimal return. However, as pointed out in the theory paper (G. Stevanato, J. Mag. Reson. **274** (2017), 148-162), this angle can be anything except 180^\circ to observe a polarization transfer.

(ii) The value of \Delta and 'm' are set according to alpha. The equations and extensive simulations are presented in the theory paper.

To stress these points, we include a sentence in theory Section 2.1, last paragraph.

*"*To keep our studies simple, in this work we employ ADAPT_{30} which experimentally we found to be optimal, however as predicted all of the combinations of \alpha, \Delta and 'm' we tested produced a return. *[Ref]"*

[3] Correct typos: KHz=>kHz and hyperpolarization=>hyperpolarization.

Typos fixed.

[4] I do not like the term "parahydrogenation". "Hydrogenation with p-H_2" would be more appropriate.

The sentence is now reordered.

==========

Reviewer #2:

1a) Would 1 kHz CW irradiation be sufficient to account for differences in susceptibility in the sample volume during bubbling?

The proposed experiment can be run also without CW irradiation. Under this condition a polarization transfer also occurs. However, we have experimentally observed that CW irradiation on the ^{1}H channel significantly increases the degree of transfer.

We have included a sentence in Section 3, 3rd paragraph to explain this.

"However, when performed without any CW pulse in proton channel, we observe polarization transfer, albeit with a 30-40 % of less enhancement than earlier."

1b) Large part of the sample volume is outside the coil region and is not subjected to RF irradiation. During the bubbling period (and, most likely, long afterwards) extensive displacement of the NMR sample outside the sample volume occurs. This is probably going to make RF irradiation ineffective. Please comment on points (a) and (b).

We are now aware of 2 references that consider this point and these are included [Barskiy *et al.*, PCCP **18** (2016), 89; Knecht *et al.*, RSC Adv. **6** (2016), 24470]. It is correct that an extensive molecular displacement probably occurs during the bubbling period and also afterwards. However, the ADAPT method itself consists of a sequence of pulses and delays recursively repeated, and there is an experimental evidence that this method achieves polarization transfer. This in itself suggests that RF irradiation is effective, although it could be entirely correct that the diffusion dynamics has an impact on the efficiency of the transfer. As pointed out in the conclusion, concentration and solvent dependence study will give a better understanding on this subject.

We have now included a sentence in Section 3, 4th paragraph.
"The \epsilon is also limited by several other factors e.g. RF inhomogeneity and imperfections caused by mixing and diffusion. [Ref, Ref]"

2) While the theoretical treatment of ADAPT is clear when applied to PHIP, the consequences of using this scheme in the presence of reversible exchange are not obvious. I would appreciate if the authors would clarify the effects of an incoherent exchange process superimposed to the coherent transfer determined by ADAPT. This is important, considering that the enhancement obtained in the presented case is several orders of magnitude lower than predicted (93% transfer) based on the theory of ADAPT.

SABRE is a coherent process that is time averaged. Here we might view the starting point as a state initiation step. The sample evolves then under chemical exchange which is time precise. The dynamics of this process will impact on the efficiency of ADAPT. A more in-depth study would indeed be needed to quantify these effects. The scope of the present article is simple to illustrate a new SABRE approach, that is capable of achieving polarization transfer in a much-reduced time compared to other schemes. Those schemes are also affected by exchange processes as described in question 2). Given the rapid nature of ADAPT such effects will be diminished here.

We have therefore added a sentence in the conclusion section.
"In the future, we plan to examine how the dynamics of SABRE exchange can be harnessed to improve this ADAPT process."

3) The maximum enhancement (almost 1000-fold) was obtained after 40 cycles of ADAPT. According to the main text: "Ultimately, spin relaxation takes over in the magnetization build-up process and starts decreasing with larger loop counts." The buildup period (1.6 s) appears to be rather short, compared to 15N T1. Could consumption of p-H2 in solution rather than spin relaxation be the reason for the buildup profile?

It is likely that the T_1 times of ^{15}N are longer and hence a longer build-up time can be employed. A paper by Barskiy *et al.*, (PCCP **18** (2016), 89)) gives support to this statement. There is a further effect based on p-H_2 consumption that should be considered. Inside the NMR tube, the amount of catalyst is 0.0064 moles whilst the amount of H_2 is 0.0856 moles. There is therefore a 13.4 fold

excess during these measurements which compares well to the values used under SABRE. *para*-H_2 consumption might therefore play a role here but it is not likely to be major.

We have now modified the sentence in Section 3, 4th paragraph.
"Ultimately, spin relaxation together with *p*-H_2 consumption take over in the magnetization build-up process and \epsilon starts decreasing with larger loop counts."

4) In the thermal 15N spectrum in figure 4b the signal of the bound substrate is not observable. Based on the reported concentrations I would expect comparable signals for the substrate in the free- and bound- form. Can you explain the absence of signal for the bound-form?

With larger thermal scans (>2000), we did indeed see signals originating from the bound-forms. However, the presented Figure consists of only 400 scans, that were found insufficient to detect clear bound-signals. As opposed to 1H SABRE signals, we do not see similar concentration ratios by integrating different forms of 15N signals. The reasons can be attributed to complex exchange process and much shorter relaxation time constants (T_1 and T_2).

We have now included a sentence in Section 3, 5th paragraph.
"The lack of a thermal signal for the bound peaks can be attributed to their broad line shapes, they are visible after 2000 scans."

5) Legend to figure 1: "The standard Iridium based metal catalyst (Ir-Imes) are used with IMes…" should be changed to "The standard Iridium based metal catalyst (Ir-Imes) is used with IMes…"

OK, changed.

Direct Enhancement of Nitrogen-15 Targets at High-field by Fast ADAPT-SABRE

Soumya S. Roy[a], Gabriele Stevanato[b], Peter J. Rayner[a], Simon B. Duckett[a,*]

[a]*Department of Chemistry, University of York, Heslington, YO10 5DD, York, United Kingdom*
[b]*Institut des Sciences et Ingénierie Chimiques, Ecole Polytechnique Fédérale de Lausanne (EPFL), Lausanne 1015, Switzerland*

Abstract

Signal Amplification by Reversible Exchange (SABRE) is an attractive nuclear spin hyperpolarization technique capable of huge sensitivity enhancement in nuclear magnetic resonance (NMR) detection. The resonance condition of SABRE hyperpolarization depends on coherent spin mixing, which can be achieved naturally at a low magnetic field. The optimum transfer field to spin-1/2 heteronuclei is technically demanding, as it requires field strengths weaker than the earth's magnetic field for efficient spin mixing. In this paper, we illustrate an approach to achieve strong ^{15}N SABRE hyperpolarization at high magnetic field by a radio frequency (RF) driven coherent transfer mechanism based on alternate pulsing and delay to achieve polarization transfer. The presented scheme is found to be highly robust and much faster than existing related methods, producing $\sim$ 3 orders of ^{15}N signal enhancement within 2 seconds of RF pulsing.

Keywords: Hyperpolarization, PHIP, SABRE, ADAPT

1. Introduction

Despite the huge success of NMR in a wide assortment of research fields ranging from structural material characterization to the imaging of internal human organs, it is still regarded to be underexploited based on its theoretical potential [1, 2]. Most of the successes of NMR and MRI applications have been achieved utilizing the thermal level of nuclear spin polarization which is only of the order of 10^{-5} at room temperature in a standard high field spectrometer [2]: only one spin over 30,000 contributes to the NMR signal for protons in a 9.4 T magnet. Improving this poor sensitivity would make NMR and MRI more widespread and cost-efficient. The solution to this quest is offered by hyperpolarization methods that enhance the nuclear spin polarization by up to 5 orders of magnitude compared to standard thermal polarization [3]. This large sensitivity enhancement enables the completion of high-end MRI applications e.g. *in vivo* study of human cancer, which could otherwise not be performed due to sensitivity issues [4, 5, 6].

Within the class of hyperpolarization techniques, the Para-hydrogen Induced Polarization (PHIP) method employs a highly ordered nuclear singlet, para-hydrogen (p-H_2) gas, to enhance poorly polarized substrate spins by several orders of magnitude [7, 8]. An important variant of the PHIP technique, SABRE was introduced in 2009, that no longer requires active hydrogenation to hyperpolarize targeted molecules [9]. It relies on the temporary association of the substrate at a metal center where the associated J-coupling network ultimately enables the generation of hyperpolarized substrates(see Fig. 1a). SABRE provides a simple, fast and cost-efficient approach to hyperpolarize substrates in its original form and they can be re-polarized several times in quick succession, providing the opportunity to achieve continuous hyperpolarization [10]. The method has been successful in polarizing a large class of biologically relevant substrates where their ^{1}H , ^{13}C and ^{15}N nuclei [11, 12, 13, 14] are senitised, and also in preparing

*Corresponding author. Address: Department of Chemistry, University of York, Heslington, YO10 5DD, York, UK, Tel: +44 1904 322564

Email addresses: soumya.roy@york.ac.uk (Soumya S. Roy), gabriele.stevanato@epfl.ch (Gabriele Stevanato), simon.duckett@york.ac.uk (Simon B. Duckett)

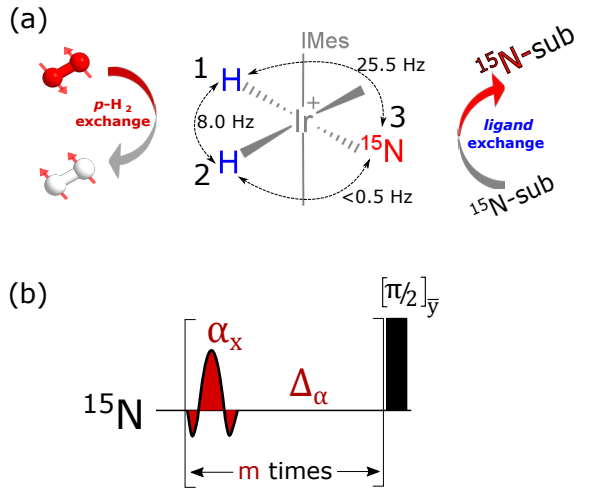

Figure 1: (a) Schematic depiction of SABRE hyperpolarization mechanism. The standard Iridium based metal catalyst (Ir-Imes) is used with IMes = 1,3-bis(2,4,6-trimethylphenyl)imidazol-2-ylidene. Singlet order from *para*-hydrogen is introduced reversibly to the hydrides, which subsequently transfer the polarization to substrate spins (^{15}N -sub) via a J-coupling network under suitable resonance conditions. (b) ADAPT pulse sequence used in this study to achieve high-field SABRE transfer.

long-lived forms that are detectable for up to 30 minutes [15, 16, 17, 18, 19]. Considering their biological relevance, hyperpolarizing spin-1/2 heteronuclei already show great importance for *in vivo* MRI studies [20, 21].

The coherent spin mixing condition for heteronuclei in SABRE can be achieved by bubbling the solution at ultra-low magnetic field (typically 0.2-1.0 μT), as previously shown by Theis *et al* [22]. However, this low-field technique requires field-cycling between low and high magnetic fields, a condition that is both technically demanding and unsuitable for immediate signal detection. Overcoming this challenge, Warren and co-workers proposed the LIGHT-SABRE approach to create a similar resonance condition at high field by applying an optimized spin-lock based RF pulse sequence [23]. Pravdivtsev *et al* have since developed a ramp based CW pulse to achieve hyperolarization in heteronuclei [24, 25].

Here we show that, the recently published ADAPT (Alternating Delays Achieve Polarization Transfer) sequence [26] can be applied to transfer polarization from singlet hydrides to target ^{15}N nuclei in a repetitive fashion. It takes only few seconds to build up strong ^{15}N hyperpolarized signal whilst the transfer mechanism being fully compatible to LIGHT-SABRE [23], Level Anti-Crossing (LAC) [27] and PHIP spin-order transfer mechanisms [28].

This article is organized as follows: In section 2 we briefly describe the ADAPT method and its optimizations by simulations yielding a SABRE perspective. In section 3 we present experimental details and results. Finally, section 4 contains conclusions and discussions.

2. Methods

2.1. ADAPT approach

We consider a system formed by three nuclear spins: two hydride ^{1}H (**1** and **2** in Fig. 1a) and a ^{15}N (**3** in Fig. 1a). The aim is to transfer nuclear spin polarization between the ^{1}H singlet spin population and ^{15}N longitudinal magnetization. ^{1}H chemical equivalence is assumed, and it is experimentally imposed by CW irradiation on the ^{1}H channel.

In a doubly rotating frame, if the ^{1}H nuclei are chemically equivalent, the J coupling terms form the coherent Hamiltonian:

$$\mathrm{H_J} = \omega_J \mathbf{I_1}\cdot\mathbf{I_2} + \frac{\omega_\Sigma+\omega_\Delta}{2} I_{1z}I_{3z} + \frac{\omega_\Sigma-\omega_\Delta}{2} I_{2z}I_{3z} \quad (1)$$

where $\omega_J = 2\pi J_{12}$, $\omega_\Sigma = 2\pi(J_{13}+J_{23})$ and $\omega_\Delta = 2\pi(J_{13}-J_{23})$. We use a basis formed by the direct product of the singlet-triplet basis for ^{1}H spins **1** and **2**, and the eigenbasis for the I_{3x} operator of ^{15}N spin **3**. In this basis, the Hamiltonian in eq. 1 can be decomposed into the direct sum of four orthogonal subspaces as detailed in ref [26]. However, we restrict the ADAPT analysis to the two relevant orthogonal subspaces $H^{\mathrm{a,b}}$ and $H^{\mathrm{c,d}}$ containing the proton singlet state:

$$H^{\mathrm{a,b}} = \begin{matrix} \\ \langle a| \\ \langle b| \end{matrix} \begin{matrix} \begin{matrix} |a\rangle & |b\rangle \end{matrix} \\ \begin{pmatrix} -\frac{3\omega_J}{4} & -\frac{\omega_\Delta}{4} \\ -\frac{\omega_\Delta}{4} & \frac{\omega_J}{4} \end{pmatrix} \end{matrix} \quad (2)$$

$$H^{\mathrm{c,d}} = \begin{matrix} \\ \langle c| \\ \langle d| \end{matrix} \begin{matrix} \begin{matrix} |c\rangle & |d\rangle \end{matrix} \\ \begin{pmatrix} \frac{\omega_J}{4} & -\frac{\omega_\Delta}{4} \\ -\frac{\omega_\Delta}{4} & -\frac{3\omega_J}{4} \end{pmatrix} \end{matrix} \quad (3)$$

where $|a\rangle = -(|S^0,\alpha\rangle - |S^0,\beta\rangle)$, $|b\rangle = (|T^0,\alpha\rangle + |T^0,\beta\rangle)$, $|c\rangle = -(|T^0,\alpha\rangle - |T^0,\beta\rangle)$ and $|d\rangle = (|S^0,\alpha\rangle + |S^0,\beta\rangle)$. The out-of-diagonal elements $-\frac{\omega_\Delta}{4}$ in eq. 2 and 3 can be exploited to transfer

polarization from $|S^0\rangle\langle S^0|$ to I_{3x}. One of such methods is the ADAPT sequence as shown in Fig. 1b. It performs the task via a number of RF pulses and delays that are recursively repeated. Small and/or large α tip angle pulses can be used, providing the experimentalist a further degree of freedom. The protocol includes a number of steps: (i) definition of the tip angle: for example $\alpha = 30°$, (ii) calculation of the conversion efficiency for a given range of delays Δ and loop numbers m as detailed in [26], (iii) choice of the optimal pair Δ_{opt} and m_{opt}. A 90° pulse at the end of the loops (see Fig. 1b), is inserted to transform I_{3x} into I_{3z} so as to retain magnetization on the substrate upon dissociation. For the present case, the J coupling network is known: $J_{12} = 8$ Hz, $J_{13} - J_{23} = 25.5$ Hz, and $J_{13} + J_{23} = 25.5$ Hz and a theoretical transfer of 93% is achieved by ADAPT_{30} in about 40 ms with $\Delta = 8$ ms and $m = 5$. In practice, multiple repetitions of this block are required to build up bulk longitudinal heteronuclear magnetization (see Fig. 5). **To keep our studies simple, in this work we employ ADAPT_{30} which experimentally we found to be optimal, however as predicted all of the combinations of α, Δ and m we tested produced a return [26].** ADAPT remains robust even in the case of uncertainty about the value of the heteronuclear J_{23} (simulations not shown).

2.2. Initial state and trajectories

When the parahydrogen and the substrate bind to the catalyst, the initial state can be represented as an overpopulation of the ^{1}H scalar singlet order. We can define a set of orthogonal operators $I_x^{rs}, I_y^{rs}, I_z^{rs}$ with cyclic commutation relationships $[I_x^{rs}, I_y^{rs}] = iI_z^{rs}$, for each of the 2×2 subspaces in eq 2 and 3. The initial state and the observable I_{3x} ^{15}N -transverse magnetization are related to the following single transitions operators:

$$|S_0\rangle\langle S_0| \propto \frac{1}{2}(I_z^{ab} - I_z^{cd})$$
$$\frac{I_{3x}}{2} \propto -\frac{1}{2}(I_z^{ab} + I_z^{cd}) \tag{4}$$

From the set of equations 4, it is apparent that polarization transfer can be obtained, for example, when a sequence of events inverts the sign of the operator I_z^{cd} while maintaining the sign of the operator I_z^{ab}. ADAPT achieves this by performing a π rotation in the subspace $H^{\text{c,d}}$ (see Fig. 2).

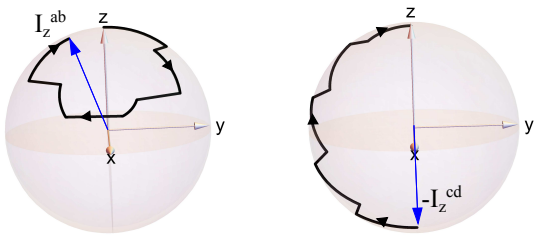

Figure 2: ADAPT induced rotations in the subspaces $H^{\text{a,b}}$ and $H^{\text{c,d}}$ upon application of ADAPT_{30} for $\Delta = 8$ ms and $m = 5$ for $J_{12} = 8$ Hz, J_{13}-$J_{23} = 25.5$ Hz.

2.3. Analogy with the LIGHT-SABRE and the LAC approach

A LAC [27] occurs when (i) the energy level relative to a pair of states $|m\rangle$ and $|n\rangle$ is equal $E_{|m\rangle} = E_{|n\rangle}$ and (ii) there is a matrix element $V_{mn} = \langle m|V|n\rangle$ for some operator V that splits them. Essentially, the LIGHT-SABRE and LAC methods share the same clever idea: a resonance condition between the spin populations of the subspaces $H^{\text{a,b}}$ and $H^{\text{c,d}}$ can be established upon spin locking on the heteronuclear channel. The Hamiltonian operator for a constant RF heteronuclear irradiation is $H_{\text{RF}} = 2\pi\nu_{\text{RF}} I_{3x}$. The ramp modulation used in the LAC method can be included by introducing a time dependency in the term ν_{RF}. For simplicity, here we disregard the time dependency ν_{RF} as in the LIGHT-SABRE protocol [23]. The matrix representation of the Hamiltonian operator $\tilde{H} = H_{\text{J}} + H_{\text{RF}}$ transforms eq. 2 and 3 into:

$$\tilde{H}^{\text{a,b}} = \begin{matrix} \\ \langle a| \\ \langle b| \end{matrix} \begin{matrix} \begin{matrix} |a\rangle & |b\rangle \end{matrix} \\ \begin{pmatrix} -\frac{3\omega_J}{4} - \pi\nu_{\text{RF}} & -\frac{\omega_\Delta}{4} \\ -\frac{\omega_\Delta}{4} & \frac{\omega_J}{4} + \pi\nu_{\text{RF}} \end{pmatrix} \end{matrix} \tag{5}$$

$$\tilde{H}^{\text{c,d}} = \begin{matrix} \\ \langle c| \\ \langle d| \end{matrix} \begin{matrix} \begin{matrix} |c\rangle & |d\rangle \end{matrix} \\ \begin{pmatrix} \frac{\omega_J}{4} - \pi\nu_{\text{RF}} & -\frac{\omega_\Delta}{4} \\ -\frac{\omega_\Delta}{4} & -\frac{3\omega_J}{4} + \pi\nu_{\text{RF}} \end{pmatrix} \end{matrix} \tag{6}$$

In equations 5 and 6, when $\nu_{\text{RF}} = J_{12}$, $E_{|a\rangle} = E_{|b\rangle} = E_{|c\rangle} = E_{|d\rangle}$ so that a level crossing occurs. More importantly, in presence of magnetic inequivalence $\omega_\Delta \neq 0$, and a LAC can be established for each subspace in eq. 5 and 6. As a result, the heteronuclear J-coupling imbalance removes the degeneracy and promotes spin population transfer in each subspace $\tilde{H}^{\text{a,b}}$ and $\tilde{H}^{\text{c,d}}$. The term ω_Δ is completely analogous to V_{mn}. The duration of the optimal spin lock is inversely proportional to $\sqrt{2}\omega_\Delta$ [23]. To

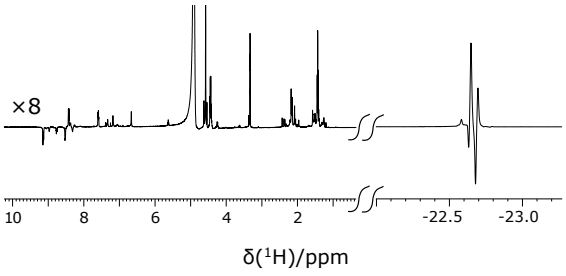

Figure 3: ^{1}H PHIP NMR spectrum of ^{15}N - ethylnicotinate measured in a 500 MHz spectrometer, showing enhanced hydride region. The coupling constants presented in Fig. 1a can be calculated from the spectrum. The 'down-field' region (0-10 ppm) is vertically multiplied by 8 compared to the 'up-field' (hydride) region.

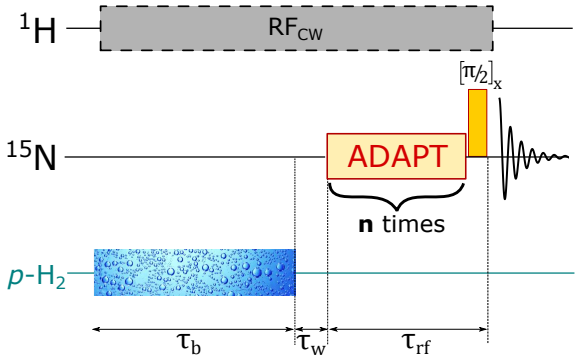

Figure 4: Experimental timings and RF sequence for the high-field ADAPT-SABRE experiment. The solution was bubbled by p-H_2 gas for the duration of τ_b; after that an appropriate waiting time (τ_w) was provided in settling down the solution before applying the ADAPT pulse sequence (as shown in Fig. 1b) in ^{15}N channel on-resonance and selectively exciting the equatorial *bound* peak. The ADAPT block was repeated n times before a final 90° hard pulse detect the signal. A low-powered continuous wave (CW) pulse was applied on ^{1}H channel throughout the experiment on-resonance to the hydrides region.

complete the analogy with the ADAPT method, it has also been noted by Theis [23], that the effect of the CW irradiation is to produce a π pulse which transfers population between the hydrogen singlet population to the ^{15}N transverse magnetization: precisely the same transformation achieved by ADAPT in the subspace of eq. 3 (see Fig. 2).

3. Experimental Results and Discussions

All the measurements were carried out with a 500 MHz Bruker Avance III spectrometer equipped with a broad-band (BBO) probe at 298 K. The sample was prepared in a 5 mm NMR tube by mixing 10 mM of [IrCl(COD)(IMes)] (IMes=1,3-bis(2,4,6-trimethylphenyl) imidazole-2-ylidene, COD=cyclooctadiene) pre-catalyst and 50 mM of ^{15}N-ethylnicotinate [29] in 0.6 ml methanol-d_4 solution. A valve-controlled p-H_2 flow PTFE (polytetrafluoroethylene) tube was immersed inside the NMR tube to bubble the solution with p-H_2 originating from a para-hydrogen generator with 90% enrichment. To accurately assign the resonances of the concerned spins and measuring their coupling constants within the network, we first performed a standard in-magnet PHIP experiment by bubbling p-H_2 inside the spectrometer and recording a ^{1}H spectrum upon applying a 45° pulse on proton channel. A large and transient antiphase spectrum is observed in the hydride region reflecting the hydrogenation product, resulting from reaction with p-H_2. Both the hydrides (spin-**1** and -**2**) show overlapping resonances at -22.66 ppm as shown in Fig. 3. The $^{2}J_{HH}$ and *cis*-$^{2}J_{NH}$ coupling constants were simply measured from the hydride region of the spectrum, whilst *trans*-$^{2}J_{NH}$ could not be observed it is expected to be negligible (< 0.5 Hz) in these types of system [12, 27].

Next we performed a standard SABRE-SHEATH experiment [22] by shaking the solution with p-H_2 inside a μ-metal can and then quickly recording a ^{15}N spectra upon a 90° detection pulse. The purpose of this experiment was to find out the ^{15}N resonance frequencies for the different forms of the substrate; the substrate can be *free* from the catalyst and also *bound* to the catalyst. Two different forms of *bound* substrate exist here (equatorial and axial position). In our study, we observe ^{15}N *free* resonance at 303.22 ppm and equatorial-*bound* resonance at 256.60 ppm whilst the axial-*bound* resonance remains undetected due to insufficient detectable polarization. The parameters obtained from these initial screening experiments were sufficient to optimize the ADAPT pulse sequence numerically (see Fig. 1b).

The high-field SABRE experiments were performed according to the experimental protocol depicted in Fig. 4. After a suitable relaxation delay, p-H_2 was bubbled through the solution for a duration of τ_b (typically 10 s) followed by a short waiting period ($\tau_w \sim 1$ s.) for the solution to settle. The optimized ADAPT pulse sequence immediately followed with a total duration of τ_{rf} ($\approx \Delta \times m \times n$),

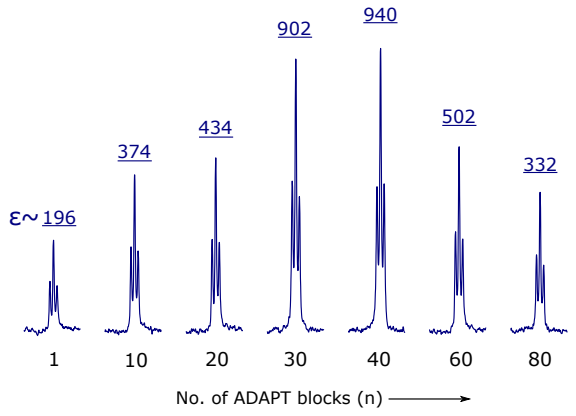

Figure 5: ADAPT-SABRE derived ^{15}N spectra showing *free* substrate peaks with increasing numbers (n) of ADAPT block (see Fig. 4). A maximum enhancement of 940-fold was achieved at n=40.

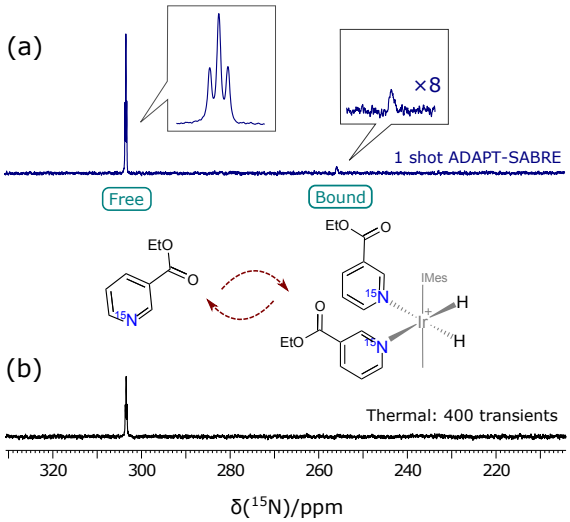

Figure 6: ^{15}N NMR spectra of ^{15}N-ethyl nicotinate showing hyperpolarized spectra acquired by ADAPT-SABRE method in seconds and (b) corresponding thermal spectra obtained by 90° hard pulses over 400 transients with 120 s of recycle delays (total experimental time of 13.5 hours). The *free* ^{15}N resonance peak was observed at 303.2 ppm whilst the 'equatorial-bound' peak was found at 255.6 ppm.

selectively exciting the *bound*-^{15}N resonance without affecting the *free* resonance. The offset for ^{15}N channel was set on the *bound*-peak (256.60 ppm) whilst the band-width (BW) of the RF pulse was kept at 500 Hz (≈10 ppm). After n number of repeated ADAPT blocks, a hard 90° pulse was applied to detect the magnetization. During the RF sequence, a continuous-wave (CW) pulse of 1 kHz band-width was applied in proton channel resonant with the hydride region to enforce chemical equivalence between the hydride protons. **However, when performed without any CW pulse in proton channel, we observe polarization transfer, albeit with a 30-40% of less enhancement than earlier.**

Using the numerically optimized parameters (see Section 2), the ADAPT sequence efficiently transfers singlet-order polarization of hydrides into longitudinal polarization of ^{15}N nuclei that are connected to the network. An optimum level of polarization can be realized for ADAPT$_{30}$ with $\Delta = 8$ ms and $m = 5$ in a total pulse duration of only 40 ms. Using these parameters, one ADAPT block achieves 196-fold enhancement factor (ϵ) for the *free* ^{15}N target. The enhancement factor (ϵ) of hyerpolarization was calculated as the ratio of the integral for the hyperpolarized signal and the integral for the thermal signal divided by the number of thermal scans. As SABRE is an exchangeable process, the polarization transfer rate is limited by the residence time of both the hydrides and the free substrate, which are in the range of 100-200 ms under standard SABRE conditions. As a result, **hydrogenation with *p*-H_2** and therefore the polarization transfer does not occur simultaneously across the entire sample volume. For this reason, the ADAPT block has to be repeated multiple times to build up ^{15}N polarization. In practice, one block of ADAPT sequence transfers only a fraction of available polarization into ^{15}N magnetization. But as long as fresh p-H_2 keeps exchanging together with non-polarized substrates, we observe accumulation in ^{15}N magnetization by repeated application of the ADAPT block. Fig. 5 presents a gradual build-up in *free* ^{15}N magnetization with increasing numbers of ADAPT blocks. A maximum enhancement of 940-fold was achieved after 40 ADAPT blocks of total duration ∼ 1.6 s. **Ultimately, spin relaxation together with *p*-H_2 consumption take over in the magnetization build-up process and ϵ starts decreasing with larger loop counts. The ϵ is also limited by several other factors e.g. RF inhomogeneity and imperfections caused by mixing and diffusion [30, 31].**

In Fig. 6 we show the success of the ADAPT-SABRE method in driving polarization from *singlet*-hydrides to *bound* ^{15}N nuclei of ethylnicotinate and enhancing the *free* ^{15}N response. The ear-

lier parameters were used to achieve the 1-shot ADAPT-SABRE spectra in Fig.6a. The corresponding thermal signal in Fig.6b was acquired by averaging 400 transients with a recycle delay of 120 s ($T_1(^{15}N) = 21.5 \pm 0.5$ s), taking over 13.5 hours. The *bound* peaks remain undetectable in the thermal measurements even after many scans signifying greater relative enhancements as predicted previously [25]. **The lack of a thermal signal for the bound peaks can be attributed to their broad line shapes, they are visible after 2000 scans.**

4. Conclusions

In summary, we have used ADAPT-SABRE to generate ^{15}N hyperpolarization at high magnetic field without the requirement of below-earth field sample mixing. The conversion is robust and faster than previously reported methods: it took only 1.6 s to reach nearly 3 orders of signal enhancement for a ^{15}N target. This method has several advantages over the low-field SABRE mechanism, e.g. constant field shuttling, unnecessary signal losses during transport. The presented scheme whilst being inherently simple, can be easily augmented to any SABRE active species and their ^{13}C, ^{19}F and ^{31}P nuclei. We are currently working on its further optimization via exchange rate, sample concentration and additive-dependence studies. **In the future, we plan to examine how the dynamics of SABRE exchange can be harnessed to improve this ADAPT process.** We believe it will be of particular importance in terms of achieving *in vivo* hyperpolarization, where sample transport poses a significant challenge to hyperpolarization based experiments.

Acknowledgements

We thank the Wellcome Trust (092506 and 098335) for funding. We thank Richard John and Fadi Ahwal for experimental help. The analysis and the simulations presented in this study make extensive use of the *SpinDynamica* code [32].

References

[1] A. Abragam, Principles of Nuclear Magnetism, Oxford University Press, 1961.
[2] R.R. Ernst, G. Bodenhausen, A. Wokaun, Principles of Nuclear Magnetic Resonance in One and Two Dimensions, Oxford University Press, Oxford, 1990.
[3] J.H. Lee, Y. Okuno, S. Cavagnero, J. Magn. Reson. 241 (2014) 18-31.
[4] K. Golman, R. in'tZandt, M. Lerche, R. Pehrson, J.H. Ardenkjaer-Larsen, Cancer Res. 66 (2006) 10855-10860.
[5] S.E. Day, M.I. Kettunen, F.A. Gallagher, D.E. Hu, M. Lerche, J. Wolber, K. Golman, J.H. Ardenkjaer-Larsen, K.M. Brindle, Nat. Med. 13 (2007) 1382-1387.
[6] P. Bhattacharya, E.Y. Chekmenev, W.H. Perman, K.C. Harris, A.P. Lin, V.A. Norton, C.T. Tan, B.D. Ross, D.P. Weitekamp, J. Magn. Reson. 186 (2007) 150-155.
[7] C.R. Bowers, D.P. Weitekamp, Phys. Rev. Lett. 57 (1986) 2645-2648.
[8] R. Eisenberg, Acc. Chem. Res. 24 (1991) 110-116.
[9] R.W. Adams, J.A. Aguilar, K.D. Atkinson, M.J. Cowley, P.I.P. Elliott, S.B. Duckett, G.G.R. Green, I.G. Khazal, J. Lopez-Serrano, D.C. Williamson, Science 323 (2009) 1708-1711.
[10] R.E. Mewis, S.B. Duckett, Acc. Chem. Res. 45 (2012) 1247-1257.
[11] H.F. Zeng, J.D. Xu, J. Gillen, M.T. McMahon, D. Artemov, J.M. Tyburn, J.A.B. Lohman, R.E. Mewis, K.D. Atkinson, G.G.R. Green, S.B. Duckett, P.C.M. van Zijl, J. Magn. Reson. 237 (2013) 73-78
[12] R.V. Shchepin, D.A. Barskiy, D.M. Mikhaylov, E.Y. Chekmenev, Bioconjugate Chem. 27 (2016) 878-882
[13] D.A. Barskiy, R.V. Shchepin, A.M. Coffey, T. Theis, W.S. Warren, B.M. Goodson, E.Y. Chekmenev, J. Am. Chem. Sci. J. Am. Chem. Soc. 138 (2016) 8080-8083.
[14] P.J. Rayner, M.J. Burns, A.M. Olaru, P. Norcott, M. Fekete, G.G.R. Green, L.A.R. Highton, R.E. Mewis, S.B. Duckett, Proc. Nat. Ac. Sci. U.S.A. 114 (2017) E3188-E3194.
[15] T. Theis *et al*, Sci. Adv. 2, (2016) e1501438.
[16] S.S. Roy, P.J. Rayner, P. Norcott, G.G.R. Green, S.B. Duckett, Phys. Chem. Chem. Phys. 18 (2016) 24905-24911.
[17] S.S. Roy, P. Norcott, P.J. Rayner, G.G.R. Green, S.B. Duckett, Angew. Chem. Int. Ed. 55 (2016) 15642-15645.
[18] S.S. Roy, P. Norcott, P.J. Rayner, G.G.R. Green, S.B. Duckett, Chem. Eur. J. 23 (2017) 10496-10500.
[19] D.A. Barskiy, R.V. Shchepin, C.P.N. Tanner, J.F.P. Colell, B.M. Goodson, T. Theis, W.S. Warren, E.Y. Chekmenev, ChemPhysChem 18 (2017) 1493-1498.
[20] S.J. Nelson et al, Sci. Transl. Med. 5 (2013) 198ra108.
[21] T.B. Rodrigues, E.M. Serrao, B.W.C. Kennedy, D.E. Hu, M.I. Kettunen, K.M. Brindle, Nat. Med. 20 (2014) 93-98.
[22] T. Theis, M.L. Truong, A.M. Coffey, R.V. Shchepin, K.W. Waddell, F. Shi, B.M. Goodson, W.S. Warren, E.Y. Chekmenev, J. Am. Chem. Soc. 137 (2015) 1404-1407.
[23] T. Theis, M.L. Truong, A.M. Coffey, E.Y. Chekmenev, W.S. Warren, J. Magn. Reson. 248 (2014) 23-26.
[24] A.N. Pravdivtsev, A.V. Yurkovskaya, H.-M. Vieth, K.L. Ivanov, J. Phys. Chem. B 119 (2015) 13619-13629.
[25] A.N. Pravdivtsev, A.V. Yurkovskaya, H. Zimmermann, H.-M. Vieth, K.L. Ivanov, RSC Adv. 5 (2015) 63615-63623.
[26] G. Stevanato, J. Magn. Reson. 274 (2017) 148-162.
[27] A.N. Pravdivtsev, A.V. Yurkovskaya, N.N. Lukzen, H.-M. Vieth, K.L. Ivanov, Phys. Chem. Chem. Phys. 16 (2014) 18707-18719.
[28] S. Bär, T. Lange, D. Leibfritz, J. Hennig, D.V. Elverfeldt, J.-B. Hövener, J. Magn. Reson. 225 (2012) 25-35.
[29] ^{15}N ethyl nicotinate was synthesised in 3 steps

beginning with the cyclisation of diethyl acetone-1,3-dicarboxylate in the presence of $HC(OEt)_3$ and $^{15}NH_4OH$. The resultant dihydroxypyridine was treated with $POCl_3$ and then underwent palladium mediated hydrogenosis to give the desired compound. Full experimental procedures and characterisation data is available from the York Data Catalogue.

[30] D.A. Barskiy, A.V. Yurkovskaya, K.L. Ivanov, K.V. Kovtunov, I.V. Koptyug, Phys. Chem. Chem. Phys. 18 (2016) 89-93.

[31] S. Knecht, A.N. Pravdivtsev, J.-B. Hövener, A.V. Yurkovskaya, K.L. Ivanov, RSC Adv. 6 (2016) 24470-24477.

[32] C. Bengs and M. H. Levitt Magn. Reson. Chem. *in press* (2017) DOI: 10.1002/mrc.4642.

Direct Enhancement of Nitrogen-15 Targets at High-field by Fast ADAPT-SABRE

Soumya S. Roy[a], Gabriele Stevanato[b], Peter J. Rayner[a], Simon B. Duckett[a,*]

[a] *Department of Chemistry, University of York, Heslington, YO10 5DD, York, United Kingdom*
[b] *Institut des Sciences et Ingénierie Chimiques, Ecole Polytechnique Fédérale de Lausanne (EPFL), Lausanne 1015, Switzerland*

Abstract

Signal Amplification by Reversible Exchange (SABRE) is an attractive nuclear spin hyperpolarization technique capable of huge sensitivity enhancement in nuclear magnetic resonance (NMR) detection. The resonance condition of SABRE hyperpolarization depends on coherent spin mixing, which can be achieved naturally at a low magnetic field. The optimum transfer field to spin-1/2 heteronuclei is technically demanding, as it requires field strengths weaker than the earth's magnetic field for efficient spin mixing. In this paper, we illustrate an approach to achieve strong ^{15}N SABRE hyperpolarization at high magnetic field by a radio frequency (RF) driven coherent transfer mechanism based on alternate pulsing and delay to achieve polarization transfer. The presented scheme is found to be highly robust and much faster than existing related methods, producing $\sim$ 3 orders of ^{15}N signal enhancement within 2 seconds of RF pulsing.

Keywords: Hyperpolarization, PHIP, SABRE, ADAPT

1. Introduction

Despite the huge success of NMR in a wide assortment of research fields ranging from structural material characterization to the imaging of internal human organs, it is still regarded to be underexploited based on its theoretical potential [1, 2]. Most of the successes of NMR and MRI applications have been achieved utilizing the thermal level of nuclear spin polarization which is only of the order of 10^{-5} at room temperature in a standard high field spectrometer [2]: only one spin over 30,000 contributes to the NMR signal for protons in a 9.4 T magnet. Improving this poor sensitivity would make NMR and MRI more widespread and cost-efficient. The solution to this quest is offered by hyperpolarization methods that enhance the nuclear spin polarization by up to 5 orders of magnitude compared to standard thermal polarization [3]. This large sensitivity enhancement enables the completion of high-end MRI applications e.g. *in vivo* study of human cancer, which could otherwise not be performed due to sensitivity issues [4, 5, 6].

Within the class of hyperpolarization techniques, the Para-hydrogen Induced Polarization (PHIP) method employs a highly ordered nuclear singlet, para-hydrogen (p-H_2) gas, to enhance poorly polarized substrate spins by several orders of magnitude [7, 8]. An important variant of the PHIP technique, SABRE was introduced in 2009, that no longer requires active hydrogenation to hyperpolarize targeted molecules [9]. It relies on the temporary association of the substrate at a metal center where the associated J-coupling network ultimately enables the generation of hyperpolarized substrates(see Fig. 1a). SABRE provides a simple, fast and cost-efficient approach to hyperpolarize substrates in its original form and they can be re-polarized several times in quick succession, providing the opportunity to achieve continuous hyperpolarization [10]. The method has been successful in polarizing a large class of biologically relevant substrates where their ^{1}H , ^{13}C and ^{15}N nuclei [11, 12, 13, 14] are senitised, and also in preparing

*Corresponding author. Address: Department of Chemistry, University of York, Heslington, YO10 5DD, York, UK, Tel: +44 1904 322564
Email addresses: soumya.roy@york.ac.uk (Soumya S. Roy), gabriele.stevanato@epfl.ch (Gabriele Stevanato), simon.duckett@york.ac.uk (Simon B. Duckett)

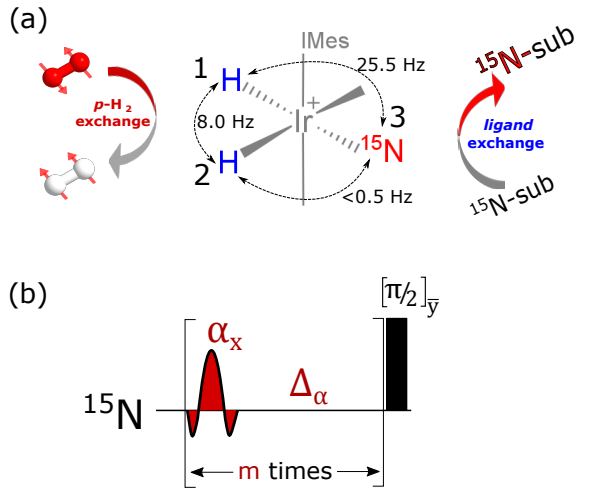

Figure 1: (a) Schematic depiction of SABRE hyperpolarization mechanism. The standard Iridium based metal catalyst (Ir-Imes) is used with IMes = 1,3-bis(2,4,6-trimethylphenyl)imidazol-2-ylidene. Singlet order from *para*-hydrogen is introduced reversibly to the hydrides, which subsequently transfer the polarization to substrate spins (^{15}N -sub) via a J-coupling network under suitable resonance conditions. (b) ADAPT pulse sequence used in this study to achieve high-field SABRE transfer.

long-lived forms that are detectable for up to 30 minutes [15, 16, 17, 18, 19]. Considering their biological relevance, hyperpolarizing spin-1/2 heteronuclei already show great importance for *in vivo* MRI studies [20, 21].

The coherent spin mixing condition for heteronuclei in SABRE can be achieved by bubbling the solution at ultra-low magnetic field (typically 0.2-1.0 μT), as previously shown by Theis *et al* [22]. However, this low-field technique requires field-cycling between low and high magnetic fields, a condition that is both technically demanding and unsuitable for immediate signal detection. Overcoming this challenge, Warren and co-workers proposed the LIGHT-SABRE approach to create a similar resonance condition at high field by applying an optimized spin-lock based RF pulse sequence [23]. Pravdivtsev *et al* have since developed a ramp based CW pulse to achieve hyperolarization in heteronuclei [24, 25].

Here we show that, the recently published ADAPT (Alternating Delays Achieve Polarization Transfer) sequence [26] can be applied to transfer polarization from singlet hydrides to target ^{15}N nuclei in a repetitive fashion. It takes only few seconds to build up strong ^{15}N hyperpolarized signal whilst the transfer mechanism being fully compatible to LIGHT-SABRE [23], Level Anti-Crossing (LAC) [27] and PHIP spin-order transfer mechanisms [28].

This article is organized as follows: In section 2 we briefly describe the ADAPT method and its optimizations by simulations yielding a SABRE perspective. In section 3 we present experimental details and results. Finally, section 4 contains conclusions and discussions.

2. Methods

2.1. ADAPT approach

We consider a system formed by three nuclear spins: two hydride ^{1}H (**1** and **2** in Fig. 1a) and a ^{15}N (**3** in Fig. 1a). The aim is to transfer nuclear spin polarization between the ^{1}H singlet spin population and ^{15}N longitudinal magnetization. ^{1}H chemical equivalence is assumed, and it is experimentally imposed by CW irradiation on the ^{1}H channel.

In a doubly rotating frame, if the ^{1}H nuclei are chemically equivalent, the J coupling terms form the coherent Hamiltonian:

$$\mathrm{H_J} = \omega_J \mathbf{I_1}\cdot\mathbf{I_2} + \frac{\omega_\Sigma+\omega_\Delta}{2} I_{1z}I_{3z} + \frac{\omega_\Sigma-\omega_\Delta}{2} I_{2z}I_{3z} \quad (1)$$

where $\omega_J = 2\pi J_{12}$, $\omega_\Sigma = 2\pi(J_{13}+J_{23})$ and $\omega_\Delta = 2\pi(J_{13}-J_{23})$. We use a basis formed by the direct product of the singlet-triplet basis for ^{1}H spins **1** and **2**, and the eigenbasis for the I_{3x} operator of ^{15}N spin **3**. In this basis, the Hamiltonian in eq. 1 can be decomposed into the direct sum of four orthogonal subspaces as detailed in ref [26]. However, we restrict the ADAPT analysis to the two relevant orthogonal subspaces $H^{\mathrm{a,b}}$ and $H^{\mathrm{c,d}}$ containing the proton singlet state:

$$H^{\mathrm{a,b}} = \begin{matrix} \\ \langle a| \\ \langle b| \end{matrix} \begin{matrix} \begin{matrix} |a\rangle & |b\rangle \end{matrix} \\ \begin{pmatrix} -\frac{3\omega_J}{4} & -\frac{\omega_\Delta}{4} \\ -\frac{\omega_\Delta}{4} & \frac{\omega_J}{4} \end{pmatrix} \end{matrix} \quad (2)$$

$$H^{\mathrm{c,d}} = \begin{matrix} \\ \langle c| \\ \langle d| \end{matrix} \begin{matrix} \begin{matrix} |c\rangle & |d\rangle \end{matrix} \\ \begin{pmatrix} \frac{\omega_J}{4} & -\frac{\omega_\Delta}{4} \\ -\frac{\omega_\Delta}{4} & -\frac{3\omega_J}{4} \end{pmatrix} \end{matrix} \quad (3)$$

where $|a\rangle = -(|S^0,\alpha\rangle - |S^0,\beta\rangle)$, $|b\rangle = (|T^0,\alpha\rangle + |T^0,\beta\rangle)$, $|c\rangle = -(|T^0,\alpha\rangle - |T^0,\beta\rangle)$ and $|d\rangle = (|S^0,\alpha\rangle + |S^0,\beta\rangle)$. The out-of-diagonal elements $-\frac{\omega_\Delta}{4}$ in eq. 2 and 3 can be exploited to transfer

polarization from $|S^0\rangle\langle S^0|$ to I_{3x}. One of such methods is the ADAPT sequence as shown in Fig. 1b. It performs the task via a number of RF pulses and delays that are recursively repeated. Small and/or large α tip angle pulses can be used, providing the experimentalist a further degree of freedom. The protocol includes a number of steps: (i) definition of the tip angle: for example $\alpha = 30°$, (ii) calculation of the conversion efficiency for a given range of delays Δ and loop numbers m as detailed in [26], (iii) choice of the optimal pair Δ_{opt} and m_{opt}. A 90° pulse at the end of the loops (see Fig. 1b), is inserted to transform I_{3x} into I_{3z} so as to retain magnetization on the substrate upon dissociation. For the present case, the J coupling network is known: $J_{12} = 8$ Hz, $J_{13} - J_{23} = 25.5$ Hz, and $J_{13} + J_{23} = 25.5$ Hz and a theoretical transfer of 93% is achieved by ADAPT_{30} in about 40 ms with $\Delta = 8$ ms and $m = 5$. In practice, multiple repetitions of this block are required to build up bulk longitudinal heteronuclear magnetization (see Fig. 5). To keep our studies simple, in this work we employ ADAPT_{30} which experimentally we found to be optimal, however as predicted all of the combinations of α, Δ and m we tested produced a return [26].

ADAPT remains robust even in the case of uncertainty about the value of the heteronuclear J_{23} (simulations not shown).

2.2. Initial state and trajectories

When the parahydrogen and the substrate bind to the catalyst, the initial state can be represented as an overpopulation of the ^{1}H scalar singlet order. We can define a set of orthogonal operators $I_x^{rs}, I_y^{rs}, I_z^{rs}$ with cyclic commutation relationships $[I_x^{rs}, I_y^{rs}] = iI_z^{rs}$, for each of the 2×2 subspaces in eq 2 and 3. The initial state and the observable I_{3x} ^{15}N -transverse magnetization are related to the following single transitions operators:

$$|S_0\rangle\langle S_0| \propto \frac{1}{2}(I_z^{ab} - I_z^{cd})$$
$$\frac{I_{3x}}{2} \propto -\frac{1}{2}(I_z^{ab} + I_z^{cd}) \qquad (4)$$

From the set of equations 4, it is apparent that polarization transfer can be obtained, for example, when a sequence of events inverts the sign of the operator I_z^{cd} while maintaining the sign of the operator I_z^{ab}. ADAPT achieves this by performing a π rotation in the subspace $H^{\text{c,d}}$ (see Fig. 2).

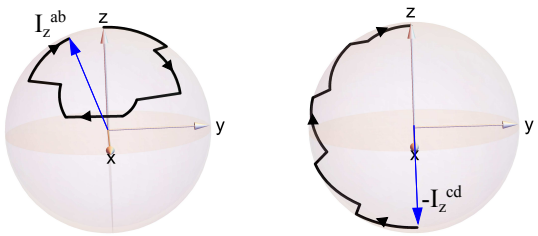

Figure 2: ADAPT induced rotations in the subspaces $H^{\text{a,b}}$ and $H^{\text{c,d}}$ upon application of ADAPT_{30} for $\Delta = 8$ ms and $m = 5$ for $J_{12} = 8$ Hz, J_{13}-$J_{23} = 25.5$ Hz.

2.3. Analogy with the LIGHT-SABRE and the LAC approach

A LAC [27] occurs when (i) the energy level relative to a pair of states $|m\rangle$ and $|n\rangle$ is equal $E_{|m\rangle} = E_{|n\rangle}$ and (ii) there is a matrix element $V_{mn} = \langle m|V|n\rangle$ for some operator V that splits them. Essentially, the LIGHT-SABRE and LAC methods share the same clever idea: a resonance condition between the spin populations of the subspaces $H^{\text{a,b}}$ and $H^{\text{c,d}}$ can be established upon spin locking on the heteronuclear channel. The Hamiltonian operator for a constant RF heteronuclear irradiation is $H_{\text{RF}} = 2\pi\nu_{\text{RF}} I_{3x}$. The ramp modulation used in the LAC method can be included by introducing a time dependency in the term ν_{RF}. For simplicity, here we disregard the time dependency ν_{RF} as in the LIGHT-SABRE protocol [23]. The matrix representation of the Hamiltonian operator $\tilde{H} = H_{\text{J}} + H_{\text{RF}}$ transforms eq. 2 and 3 into:

$$\tilde{H}^{\text{a,b}} = \begin{matrix} \\ \langle a| \\ \langle b| \end{matrix} \begin{matrix} \begin{matrix} |a\rangle & \quad |b\rangle \end{matrix} \\ \begin{pmatrix} -\frac{3\omega_J}{4} - \pi\nu_{\text{RF}} & -\frac{\omega_\Delta}{4} \\ -\frac{\omega_\Delta}{4} & \frac{\omega_J}{4} + \pi\nu_{\text{RF}} \end{pmatrix} \end{matrix} \qquad (5)$$

$$\tilde{H}^{\text{c,d}} = \begin{matrix} \\ \langle c| \\ \langle d| \end{matrix} \begin{matrix} \begin{matrix} |c\rangle & \quad |d\rangle \end{matrix} \\ \begin{pmatrix} \frac{\omega_J}{4} - \pi\nu_{\text{RF}} & -\frac{\omega_\Delta}{4} \\ -\frac{\omega_\Delta}{4} & -\frac{3\omega_J}{4} + \pi\nu_{\text{RF}} \end{pmatrix} \end{matrix} \qquad (6)$$

In equations 5 and 6, when $\nu_{\text{RF}} = J_{12}$, $E_{|a\rangle} = E_{|b\rangle} = E_{|c\rangle} = E_{|d\rangle}$ so that a level crossing occurs. More importantly, in presence of magnetic inequivalence $\omega_\Delta \neq 0$, and a LAC can be established for each subspace in eq. 5 and 6. As a result, the heteronuclear J-coupling imbalance removes the degeneracy and promotes spin population transfer in each subspace $\tilde{H}^{\text{a,b}}$ and $\tilde{H}^{\text{c,d}}$. The term ω_Δ is completely analogous to V_{mn}. The duration of the optimal spin lock is inversely proportional to $\sqrt{2}\omega_\Delta$ [23]. To

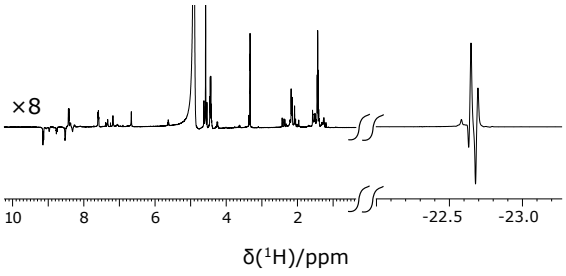

Figure 3: ^{1}H PHIP NMR spectrum of ^{15}N - ethylnicotinate measured in a 500 MHz spectrometer, showing enhanced hydride region. The coupling constants presented in Fig. 1a can be calculated from the spectrum. The 'down-field' region (0-10 ppm) is vertically multiplied by 8 compared to the 'up-field' (hydride) region.

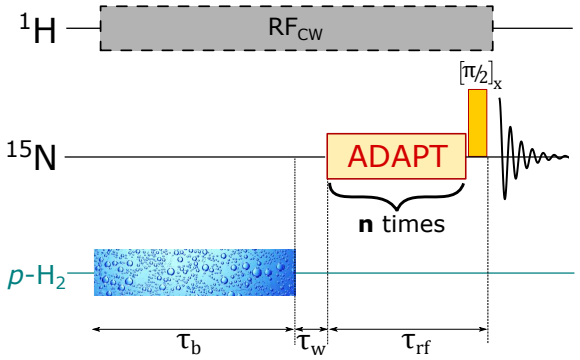

Figure 4: Experimental timings and RF sequence for the high-field ADAPT-SABRE experiment. The solution was bubbled by p-H_2 gas for the duration of τ_b; after that an appropriate waiting time (τ_w) was provided in settling down the solution before applying the ADAPT pulse sequence (as shown in Fig. 1b) in ^{15}N channel on-resonance and selectively exciting the equatorial *bound* peak. The ADAPT block was repeated n times before a final 90° hard pulse detect the signal. A low-powered continuous wave (CW) pulse was applied on ^{1}H channel throughout the experiment on-resonance to the hydrides region.

complete the analogy with the ADAPT method, it has also been noted by Theis [23], that the effect of the CW irradiation is to produce a π pulse which transfers population between the hydrogen singlet population to the ^{15}N transverse magnetization: precisely the same transformation achieved by ADAPT in the subspace of eq. 3 (see Fig. 2).

3. Experimental Results and Discussions

All the measurements were carried out with a 500 MHz Bruker Avance III spectrometer equipped with a broad-band (BBO) probe at 298 K. The sample was prepared in a 5 mm NMR tube by mixing 10 mM of [IrCl(COD)(IMes)] (IMes=1,3-bis(2,4,6-trimethylphenyl) imidazole-2-ylidene, COD=cyclooctadiene) pre-catalyst and 50 mM of ^{15}N-ethylnicotinate [29] in 0.6 ml methanol-d_4 solution. A valve-controlled p-H_2 flow PTFE (polytetrafluoroethylene) tube was immersed inside the NMR tube to bubble the solution with p-H_2 originating from a para-hydrogen generator with 90% enrichment. To accurately assign the resonances of the concerned spins and measuring their coupling constants within the network, we first performed a standard in-magnet PHIP experiment by bubbling p-H_2 inside the spectrometer and recording a ^{1}H spectrum upon applying a 45° pulse on proton channel. A large and transient antiphase spectrum is observed in the hydride region reflecting the hydrogenation product, resulting from reaction with p-H_2. Both the hydrides (spin-**1** and -**2**) show overlapping resonances at -22.66 ppm as shown in Fig. 3. The $^{2}J_{HH}$ and *cis*-$^{2}J_{NH}$ coupling constants were simply measured from the hydride region of the spectrum, whilst *trans*-$^{2}J_{NH}$ could not be observed it is expected to be negligible (< 0.5 Hz) in these types of system [12, 27].

Next we performed a standard SABRE-SHEATH experiment [22] by shaking the solution with p-H_2 inside a μ-metal can and then quickly recording a ^{15}N spectra upon a 90° detection pulse. The purpose of this experiment was to find out the ^{15}N resonance frequencies for the different forms of the substrate; the substrate can be *free* from the catalyst and also *bound* to the catalyst. Two different forms of *bound* substrate exist here (equatorial and axial position). In our study, we observe ^{15}N *free* resonance at 303.22 ppm and equatorial-*bound* resonance at 256.60 ppm whilst the axial-*bound* resonance remains undetected due to insufficient detectable polarization. The parameters obtained from these initial screening experiments were sufficient to optimize the ADAPT pulse sequence numerically (see Fig. 1b).

The high-field SABRE experiments were performed according to the experimental protocol depicted in Fig. 4. After a suitable relaxation delay, p-H_2 was bubbled through the solution for a duration of τ_b (typically 10 s) followed by a short waiting period ($\tau_w \sim 1$ s.) for the solution to settle. The optimized ADAPT pulse sequence immediately followed with a total duration of τ_{rf} ($\approx \Delta \times m \times n$),

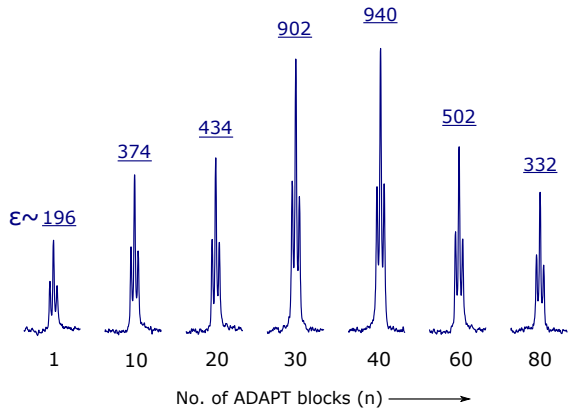

Figure 5: ADAPT-SABRE derived ^{15}N spectra showing *free* substrate peaks with increasing numbers (n) of ADAPT block (see Fig. 4). A maximum enhancement of 940-fold was achieved at n=40.

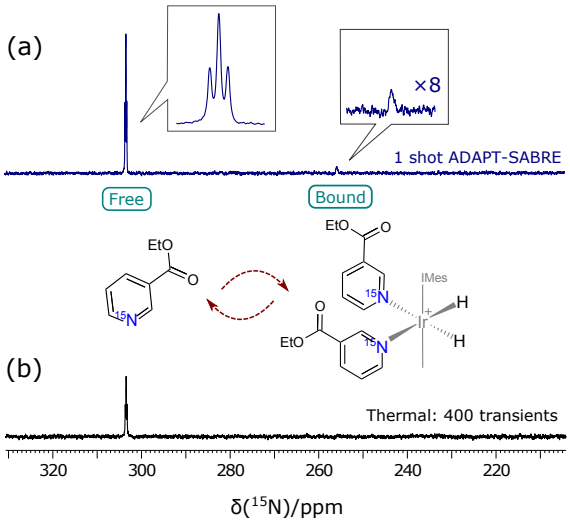

Figure 6: ^{15}N NMR spectra of ^{15}N-ethyl nicotinate showing hyperpolarized spectra acquired by ADAPT-SABRE method in seconds and (b) corresponding thermal spectra obtained by 90° hard pulses over 400 transients with 120 s of recycle delays (total experimental time of 13.5 hours). The *free* ^{15}N resonance peak was observed at 303.2 ppm whilst the 'equatorial-bound' peak was found at 255.6 ppm.

selectively exciting the *bound*-^{15}N resonance without affecting the *free* resonance. The offset for ^{15}N channel was set on the *bound*-peak (256.60 ppm) whilst the band-width (BW) of the RF pulse was kept at 500 Hz (≈10 ppm). After n number of repeated ADAPT blocks, a hard 90° pulse was applied to detect the magnetization. During the RF sequence, a continuous-wave (CW) pulse of 1 kHz band-width was applied in proton channel resonant with the hydride region to enforce chemical equivalence between the hydride protons. However, when performed without any CW pulse in proton channel, we observe polarization transfer, albeit with a 30-40% of less enhancement than earlier.

Using the numerically optimized parameters (see Section 2), the ADAPT sequence efficiently transfers singlet-order polarization of hydrides into longitudinal polarization of ^{15}N nuclei that are connected to the network. An optimum level of polarization can be realized for ADAPT$_{30}$ with $\Delta = 8$ ms and $m = 5$ in a total pulse duration of only 40 ms. Using these parameters, one ADAPT block achieves 196-fold enhancement factor (ϵ) for the *free* ^{15}N target. The enhancement factor (ϵ) of hyerpolarization was calculated as the ratio of the integral for the hyperpolarized signal and the integral for the thermal signal divided by the number of thermal scans. As SABRE is an exchangeable process, the polarization transfer rate is limited by the residence time of both the hydrides and the free substrate, which are in the range of 100-200 ms under standard SABRE conditions. As a result, hydrogenation with p-H_2 and therefore the polarization transfer does not occur simultaneously across the entire sample volume. For this reason, the ADAPT block has to be repeated multiple times to build up ^{15}N polarization. In practice, one block of ADAPT sequence transfers only a fraction of available polarization into ^{15}N magnetization. But as long as fresh p-H_2 keeps exchanging together with non-polarized substrates, we observe accumulation in ^{15}N magnetization by repeated application of the ADAPT block. Fig. 5 presents a gradual build-up in *free* ^{15}N magnetization with increasing numbers of ADAPT blocks. A maximum enhancement of 940-fold was achieved after 40 ADAPT blocks of total duration ∼ 1.6 s. Ultimately, spin relaxation together with p-H_2 consumption take over in the magnetization build-up process and ϵ starts decreasing with larger loop counts. The ϵ is also limited by several other factors e.g. RF inhomogeneity and imperfections caused by mixing and diffusion [30, 31].

In Fig. 6 we show the success of the ADAPT-SABRE method in driving polarization from *singlet*-hydrides to *bound* ^{15}N nuclei of ethylnicotinate and enhancing the *free* ^{15}N response. The earlier parameters were used to achieve the 1-shot ADAPT-SABRE spectra in Fig.6a. The correspon-

ding thermal signal in Fig.6b was acquired by averaging 400 transients with a recycle delay of 120 s ($T_1(^{15}N) = 21.5 \pm 0.5$ s), taking over 13.5 hours. The *bound* peaks remain undetectable in the thermal measurements even after many scans signifying greater relative enhancements as predicted previously [25]. The lack of a thermal signal for the bound peaks can be attributed to their broad line shapes, they are visible after 2000 scans.

4. Conclusions

In summary, we have used ADAPT-SABRE to generate ^{15}N hyperpolarization at high magnetic field without the requirement of below-earth field sample mixing. The conversion is robust and faster than previously reported methods: it took only 1.6 s to reach nearly 3 orders of signal enhancement for a ^{15}N target. This method has several advantages over the low-field SABRE mechanism, e.g. constant field shuttling, unnecessary signal losses during transport. The presented scheme whilst being inherently simple, can be easily augmented to any SABRE active species and their ^{13}C, ^{19}F and ^{31}P nuclei. We are currently working on its further optimization via exchange rate, sample concentration and additive-dependence studies. In the future, we plan to examine how the dynamics of SABRE exchange can be harnessed to improve this ADAPT process. We believe it will be of particular importance in terms of achieving *in vivo* hyperpolarization, where sample transport poses a significant challenge to hyperpolarization based experiments.

Acknowledgements

We thank the Wellcome Trust (092506 and 098335) for funding. We thank Richard John and Fadi Ahwal for experimental help. The analysis and the simulations presented in this study make extensive use of the *SpinDynamica* code [32].

References

[1] A. Abragam, Principles of Nuclear Magnetism, Oxford University Press, 1961.
[2] R.R. Ernst, G. Bodenhausen, A. Wokaun, Principles of Nuclear Magnetic Resonance in One and Two Dimensions, Oxford University Press, Oxford, 1990.
[3] J.H. Lee, Y. Okuno, S. Cavagnero, J. Magn. Reson. 241 (2014) 18-31.
[4] K. Golman, R. in'tZandt, M. Lerche, R. Pehrson, J.H. Ardenkjaer-Larsen, Cancer Res. 66 (2006) 10855-10860.
[5] S.E. Day, M.I. Kettunen, F.A. Gallagher, D.E. Hu, M. Lerche, J. Wolber, K. Golman, J.H. Ardenkjaer-Larsen, K.M. Brindle, Nat. Med. 13 (2007) 1382-1387.
[6] P. Bhattacharya, E.Y. Chekmenev, W.H. Perman, K.C. Harris, A.P. Lin, V.A. Norton, C.T. Tan, B.D. Ross, D.P. Weitekamp, J. Magn. Reson. 186 (2007) 150-155.
[7] C.R. Bowers, D.P. Weitekamp, Phys. Rev. Lett. 57 (1986) 2645-2648.
[8] R. Eisenberg, Acc. Chem. Res. 24 (1991) 110-116.
[9] R.W. Adams, J.A. Aguilar, K.D. Atkinson, M.J. Cowley, P.I.P. Elliott, S.B. Duckett, G.G.R. Green, I.G. Khazal, J. Lopez-Serrano, D.C. Williamson, Science 323 (2009) 1708-1711.
[10] R.E. Mewis, S.B. Duckett, Acc. Chem. Res. 45 (2012) 1247-1257.
[11] H.F. Zeng, J.D. Xu, J. Gillen, M.T. McMahon, D. Artemov, J.M. Tyburn, J.A.B. Lohman, R.E. Mewis, K.D. Atkinson, G.G.R. Green, S.B. Duckett, P.C.M. van Zijl, J. Magn. Reson. 237 (2013) 73-78
[12] R.V. Shchepin, D.A. Barskiy, D.M. Mikhaylov, E.Y. Chekmenev, Bioconjugate Chem. 27 (2016) 878-882
[13] D.A. Barskiy, R.V. Shchepin, A.M. Coffey, T. Theis, W.S. Warren, B.M. Goodson, E.Y. Chekmenev, J. Am. Chem. Sci. J. Am. Chem. Soc. 138 (2016) 8080-8083.
[14] P.J. Rayner, M.J. Burns, A.M. Olaru, P. Norcott, M. Fekete, G.G.R. Green, L.A.R. Highton, R.E. Mewis, S.B. Duckett, Proc. Nat. Ac. Sci. U.S.A. 114 (2017) E3188-E3194.
[15] T. Theis *et al*, Sci. Adv. 2, (2016) e1501438.
[16] S.S. Roy, P.J. Rayner, P. Norcott, G.G.R. Green, S.B. Duckett, Phys. Chem. Chem. Phys. 18 (2016) 24905-24911.
[17] S.S. Roy, P. Norcott, P.J. Rayner, G.G.R. Green, S.B. Duckett, Angew. Chem. Int. Ed. 55 (2016) 15642-15645.
[18] S.S. Roy, P. Norcott, P.J. Rayner, G.G.R. Green, S.B. Duckett, Chem. Eur. J. 23 (2017) 10496-10500.
[19] D.A. Barskiy, R.V. Shchepin, C.P.N. Tanner, J.F.P. Colell, B.M. Goodson, T. Theis, W.S. Warren, E.Y. Chekmenev, ChemPhysChem 18 (2017) 1493-1498.
[20] S.J. Nelson et al, Sci. Transl. Med. 5 (2013) 198ra108.
[21] T.B. Rodrigues, E.M. Serrao, B.W.C. Kennedy, D.E. Hu, M.I. Kettunen, K.M. Brindle, Nat. Med. 20 (2014) 93-98.
[22] T. Theis, M.L. Truong, A.M. Coffey, R.V. Shchepin, K.W. Waddell, F. Shi, B.M. Goodson, W.S. Warren, E.Y. Chekmenev, J. Am. Chem. Soc. 137 (2015) 1404-1407.
[23] T. Theis, M.L. Truong, A.M. Coffey, E.Y. Chekmenev, W.S. Warren, J. Magn. Reson. 248 (2014) 23-26.
[24] A.N. Pravdivtsev, A.V. Yurkovskaya, H.-M. Vieth, K.L. Ivanov, J. Phys. Chem. B 119 (2015) 13619-13629.
[25] A.N. Pravdivtsev, A.V. Yurkovskaya, H. Zimmermann, H.-M. Vieth, K.L. Ivanov, RSC Adv. 5 (2015) 63615-63623.
[26] G. Stevanato, J. Magn. Reson. 274 (2017) 148-162.
[27] A.N. Pravdivtsev, A.V. Yurkovskaya, N.N. Lukzen, H.-M. Vieth, K.L. Ivanov, Phys. Chem. Chem. Phys. 16 (2014) 18707-18719.
[28] S. Bär, T. Lange, D. Leibfritz, J. Hennig, D.V. Elverfeldt, J.-B. Hövener, J. Magn. Reson. 225 (2012) 25-35.
[29] ^{15}N ethyl nicotinate was synthesised in 3 steps beginning with the cyclisation of diethyl acetone-1,3-dicarboxylate in the presence of $HC(OEt)_3$ and $^{15}NH_4OH$. The resultant dihydroxypyridine was treated with $POCl_3$ and then underwent palladium medi-

ated hydrogenosis to give the desired compound. Full experimental procedures and characterisation data is available from the York Data Catalogue.
[30] D.A. Barskiy, A.V. Yurkovskaya, K.L. Ivanov, K.V. Kovtunov, I.V. Koptyug, Phys. Chem. Chem. Phys. 18 (2016) 89-93.
[31] S. Knecht, A.N. Pravdivtsev, J.-B. Hövener, A.V. Yurkovskaya, K.L. Ivanov, RSC Adv. 6 (2016) 24470-24477.
[32] C. Bengs and M. H. Levitt Magn. Reson. Chem. *in press* (2017) DOI: 10.1002/mrc.4642.

Figure1

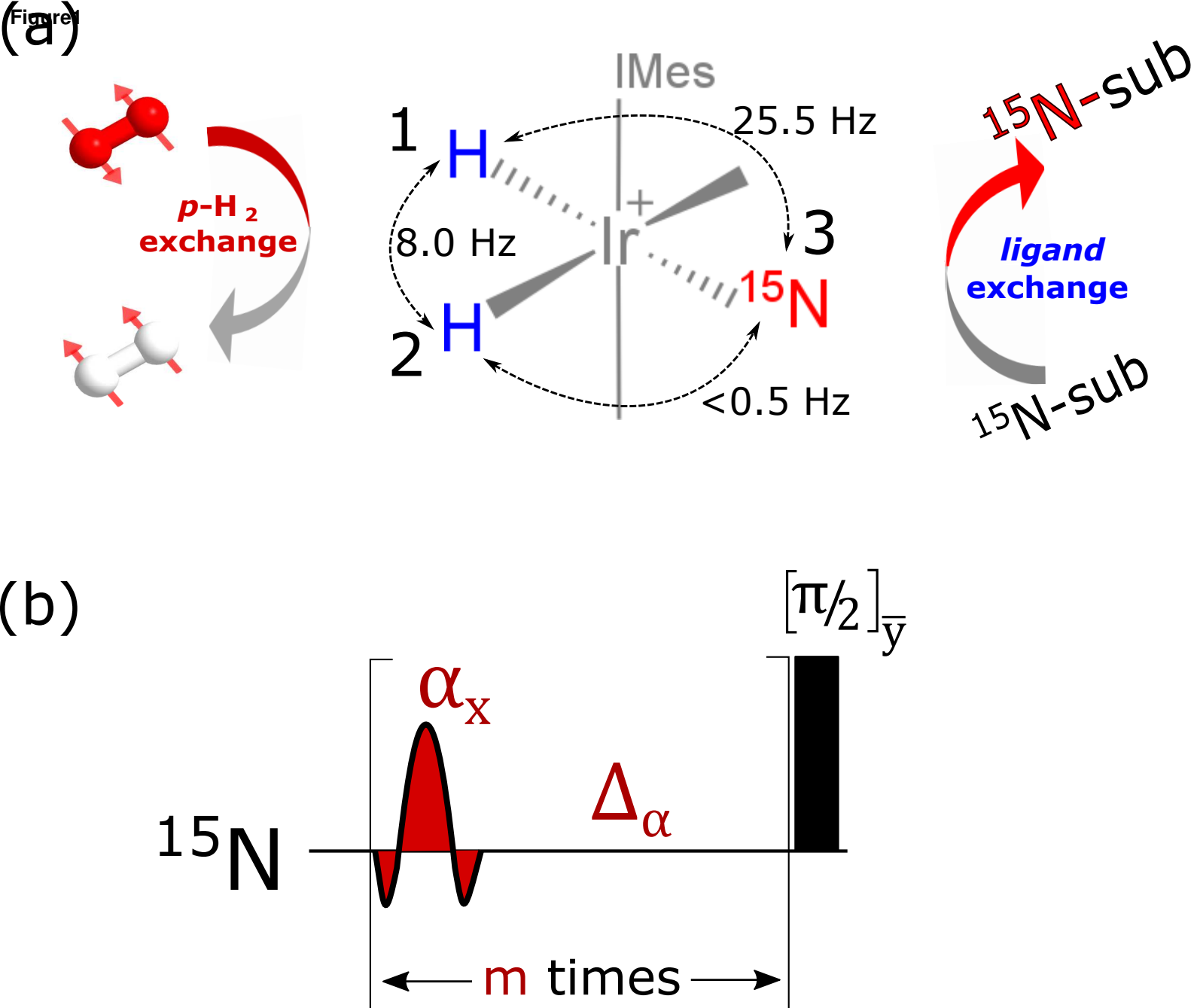
(a)
p-H 2
exchange
IMes
1
H
25.5 Hz
8.0 Hz
Ir
3
15N
2
H
<0.5 Hz
15N-sub
ligand
exchange
15N-sub
(b)
[π/2]y
αx
Δα
15N
m times

Figure2

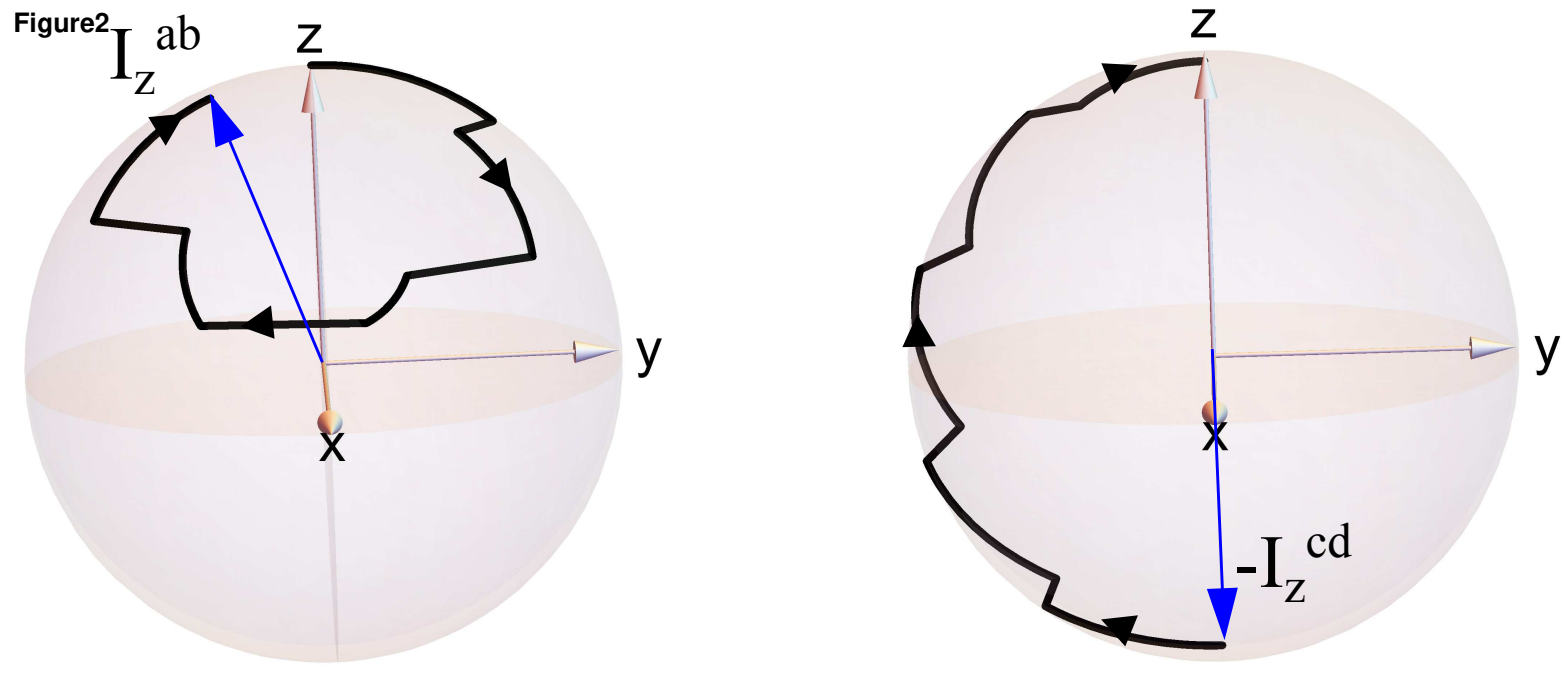

Figure3

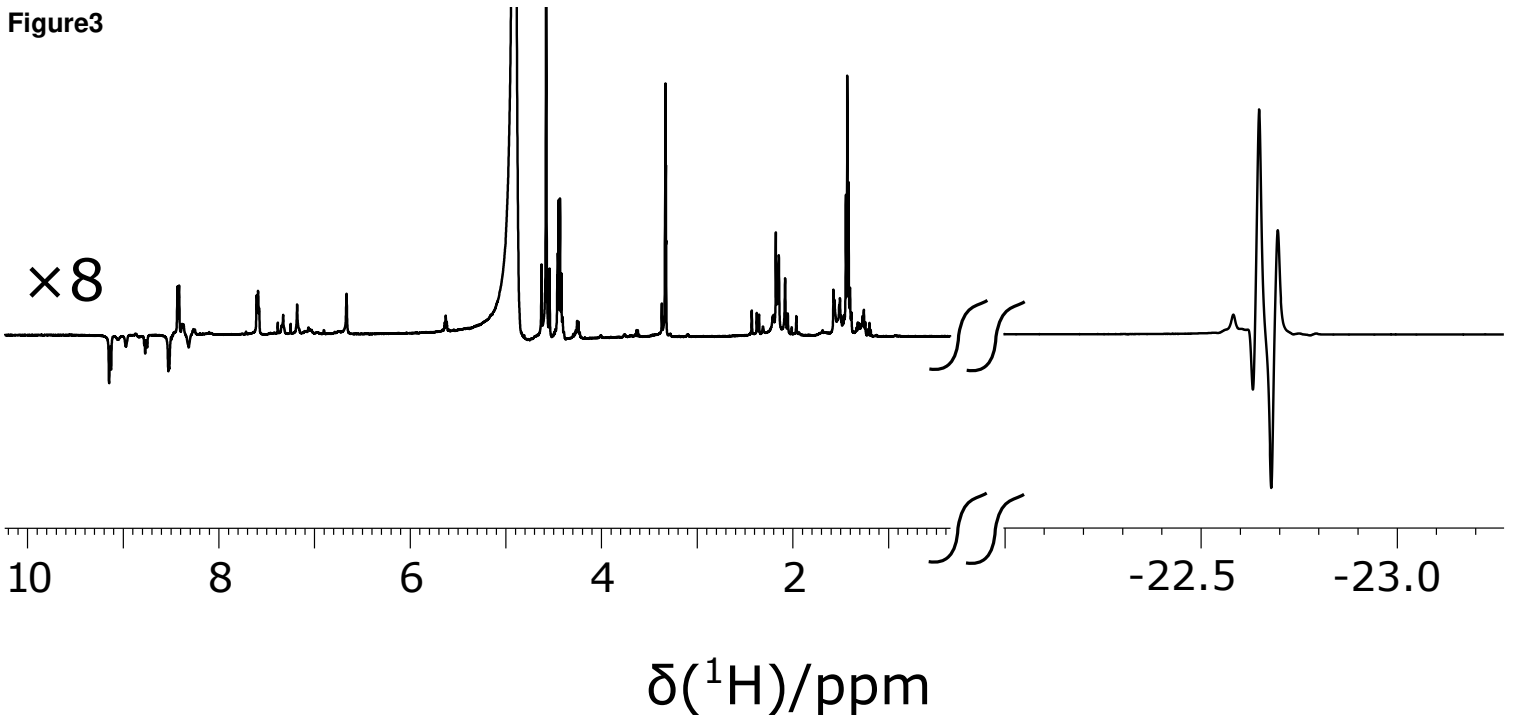

Figure4

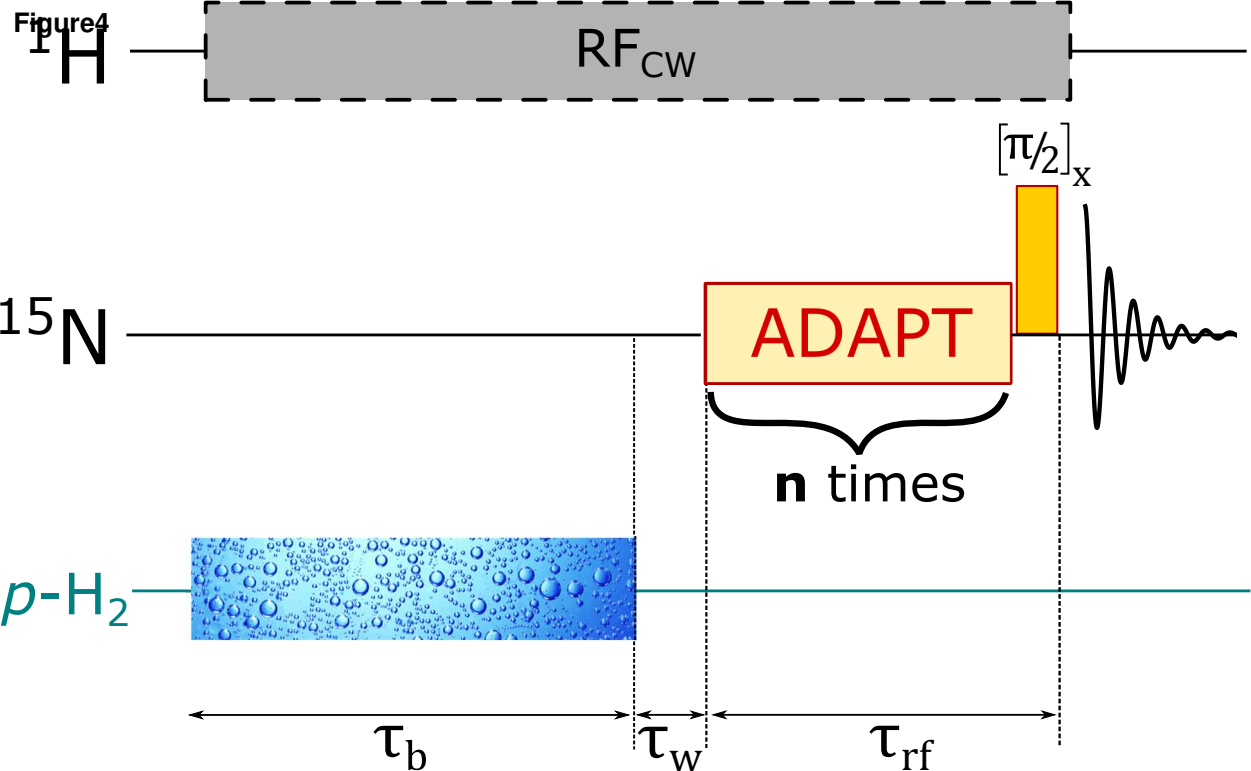

Figure5

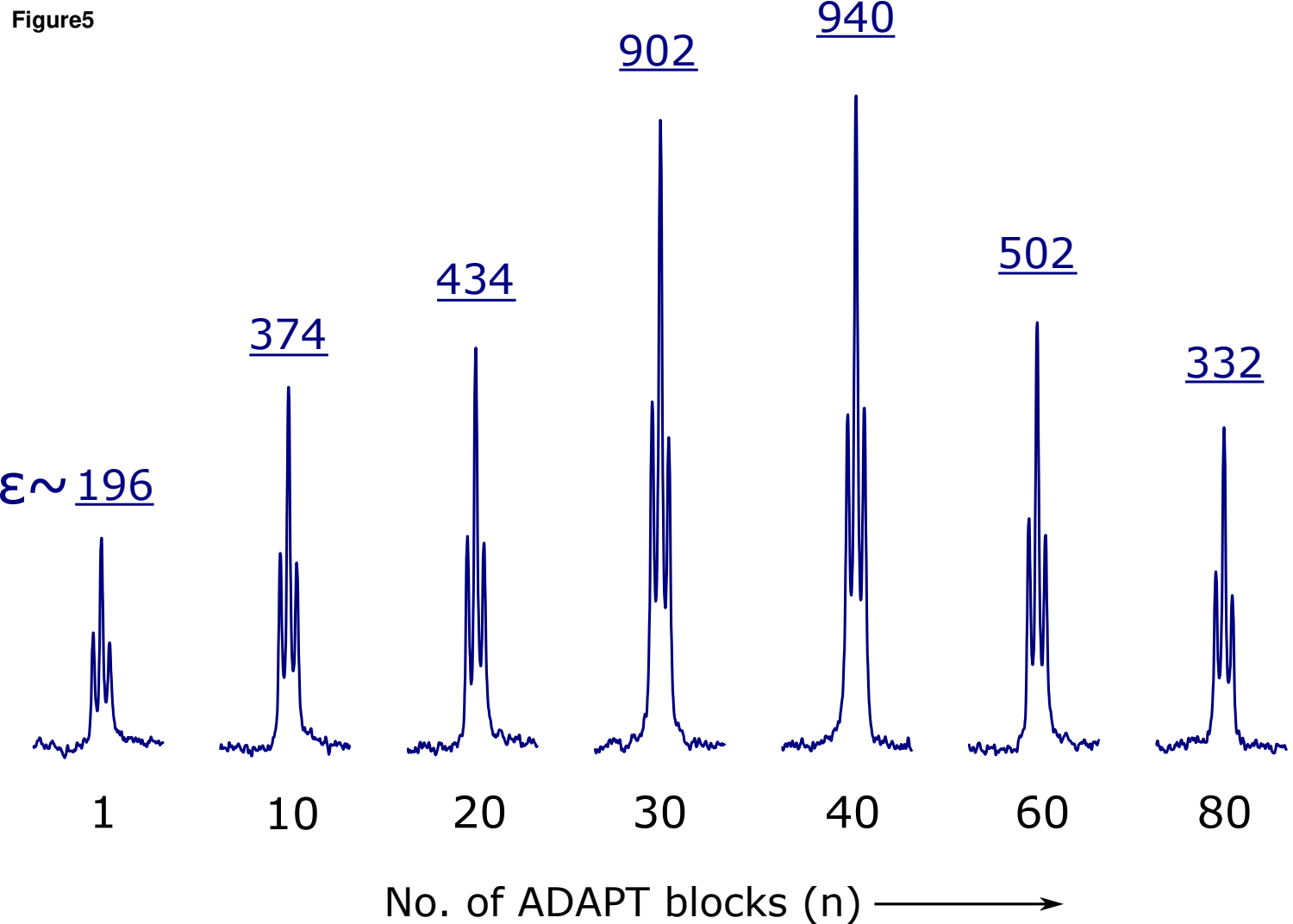
ε~196
374
434
902
940
502
332
1
10
20
30
40
60
80
No. of ADAPT blocks (n)

Figure6

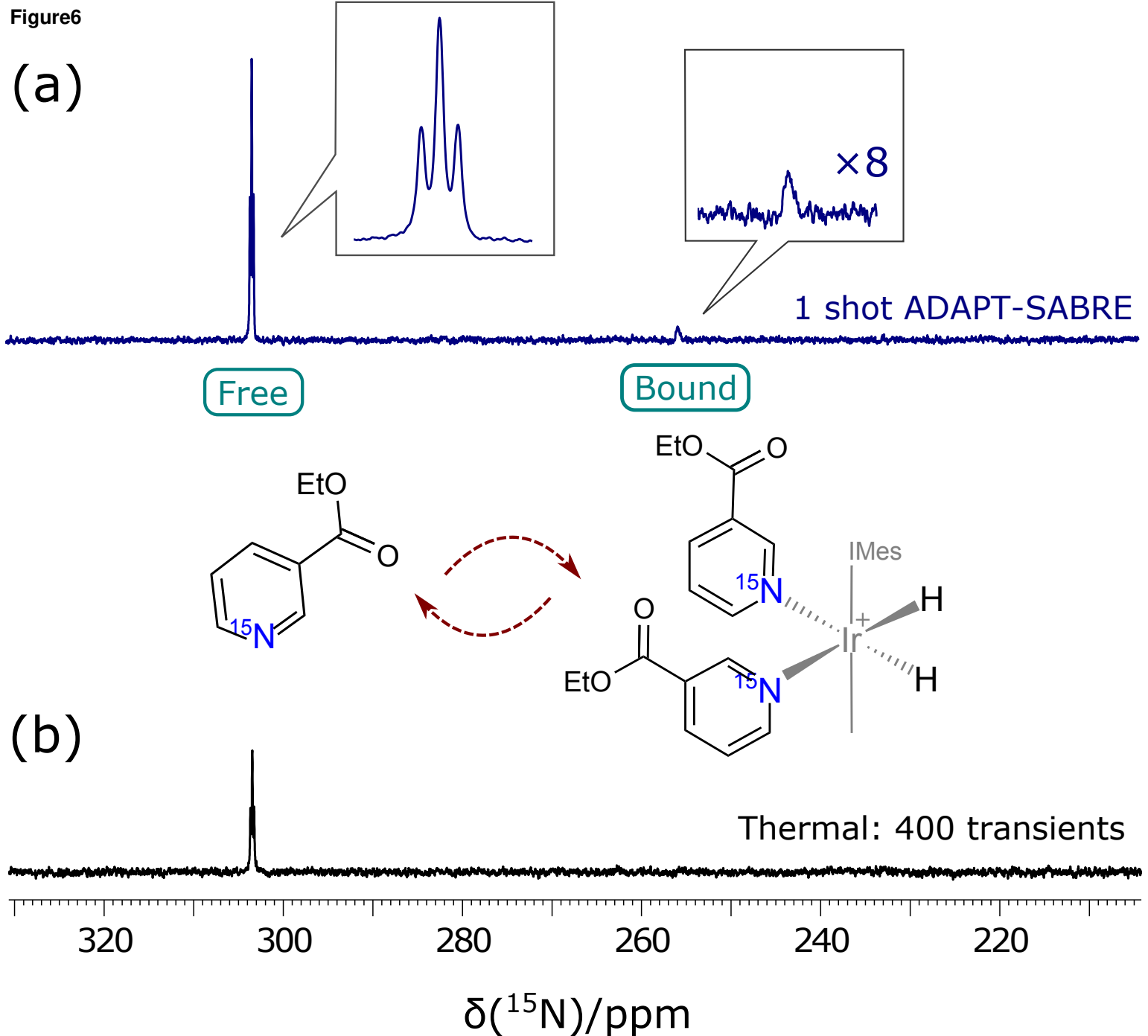
(a)
×8
1 shot ADAPT-SABRE
Free
Bound
EtO
O
15N
IMes
H
Ir
(b)
Thermal: 400 transients
320
300
280
260
240
220
δ(15N)/ppm